Multiply charged anionic metal clusters

C. Yannouleas and Uzi Landman
School of Physics, Georgia Institute of Technology, Atlanta, GA 30332-0430, USA

Received 28 April 1993

The stability and decay channels of multiply charged anionic metal clusters are studied using the uniform jellium background model and the local density approximation, with self-interaction corrections when necessary. Shell effects are introduced using an adaptation of the nuclear Strutinsky method. Singly charged anions are stable for all sizes, but multiply charged negative ions are stable against spontaneous electron decay only above certain critical sizes. Below the border of stability, the anions are metastable against electron tunneling through a Coulombic barrier. Lifetimes for such decay processes are estimated. Fission channels may compete with the electron autodetachment and are studied for the case of doubly charged anions.

1. Introduction

Charging of large metal spheres is an old subject with scientific accounts dating back to Coulomb, Faraday and others [1]. While size-evolutionary patterns of physical and chemical properties of finite clusters, neutral as well as cationic, have been the subject of intense research [2,3] [#1], multiply negatively charged metal clusters have not been much investigated [#2], perhaps because of technical experimental and theoretical difficulties.

We report on systematic theoretical studies of the energetics, stability and fragmentation channels of multiply charged anionic metal clusters. Specifically, we deduce relationships predicting borders of stability as a function of size and number of excess electrons (the cluster size required to stably bind a given number of excess electrons). Beyond the border of stability, we estimate the lifetimes for spontaneous electron emission (autodetachment) which takes place via tunneling through a Coulombic barrier, in analogy with the nuclear processes of proton and alpha radioactivities. Additionally, we assess the importance of shell effects and self-interaction corrections for anionic metal clusters studied by the local-density-functional (LDA) method within the framework of both spherical and *triaxially* (ellipsoidally) deformed jellium droplets.

[#1] For a study of multiply charged cationic clusters, see ref. [4] or also ref. [5].

[#2] For a recent review of singly charged anionic metal clusters, see ref. [6]. For some previous theoretical considerations of multiply charged anions, see ref. [32].

2. Shell-correction method

Metal clusters have been investigated extensively using local-density-functional methods and self-consistent solutions of the Kohn–Sham (KS) equations [2,7–11]. However, even for singly negatively charged metal clusters (M_N^-), difficulties may arise due to the failure of the solutions of the KS equations to converge, since the eigenvalue of the excess electron may iterate to a positive energy [12]. While such difficulties are alleviated for M_N^- clusters via self-interaction corrections (SIC) [10,11], the treatment of multiply charged clusters (M_N^{Z-}, $Z>1$) would face similar difficulties in the metastability region against electronic autodetachment through a Coulombic barrier.

An alternative LDA method, which has been used in studies of metal clusters [13–15], is based on an extended Thomas–Fermi (ETF) variational procedure using a parametrized density profile $\rho(\boldsymbol{r}; \{\gamma_i\})$, with $\{\gamma_i\}$ as variational parameters [13,14]. The energy density functional that is variationally minimized consists of a kinetic-energy functional $T[\rho]$,

comprising terms up to fourth order in the density gradients [16], and of Hartree and exchange-correlation functionals (for the latter we use the Gunnarsson–Lundqvist functional [17]). The effective potentials and associated single-particle energy spectra obtained by this method provide an excellent approximation to the corresponding ones obtained from KS calculations, and have been used extensively [15] in studies of the optical properties of metal clusters.

However, other ETF properties investigated as a function of the size of the cluster, such as ionization potentials (IPs), electron affinities (EAs) and total energies, compare with the KS values only in an average sense, i.e. they do not exhibit shell-closure effects [13,14]. In the nuclear physics literature [18], this average level of approximation is referred to as describing only the "*smooth*" part of the size dependence of the properties of a finite system. In our study, shell effects are incorporated by adapting the Strutinsky method [19,20], which has been used previously for shell corrections to the nuclear liquid-drop model. Thus shell effects in the total energy of a metal cluster are contained, to first order in $\delta\rho_{KS}$ (where $\delta\rho_{KS}=\tilde{\rho}-\rho_{KS}$, $\tilde{\rho}$ is the smooth ETF density, and ρ_{KS} is the self-consistent KS density), in the sum $\sum_i \tilde{\epsilon}_i$, where $\tilde{\epsilon}_i$ are the single-particle energies of the ETF effective potential. Accordingly, we replace the kinetic-energy $\tilde{T}$ in the ETF functional by

$$T_{sh}=\sum_i \tilde{\epsilon}_i-\int \tilde{\rho}(r)\tilde{V}(r;\tilde{\rho}(r))\,dr,$$

where $\tilde{V}(r;\tilde{\rho}(r))$ is the effective potential produced by the ETF method. As a result, the total energy, E_{sh}, including the shell correction, $\Delta E_{sh}=T_{sh}-\tilde{T}$, is given by $E_{sh}[\tilde{\rho}]=T_{sh}-\tilde{T}+\tilde{E}[\tilde{\rho}]$, where $\tilde{E}$ is the ETF energy-density functional.

After some rearrangements, the shell-correction total energy $E_{sh}[\tilde{\rho}]$ can be written in functional form as follows:

$$E_{sh}[\tilde{\rho}]=\sum_i \tilde{\epsilon}_i-\int\{\tfrac{1}{2}\tilde{V}_H(r)+\tilde{V}_{xc}(r)\}\tilde{\rho}(r)\,dr$$

$$+\int \tilde{\mathscr{E}}_{xc}[\tilde{\rho}(r)]\,dr+E_I,$$

where $\tilde{V}_H$ and $\tilde{V}_{xc}$ are the Hartree and exchange-correlation electronic potentials, $\tilde{\mathscr{E}}_{xc}$ is the exchange-correlation energy density functional and E_I is the energy of the positive jellium background. The specific way of writing the functional E_{sh} above was chosen so that its similarity in form to the Harris functional [21–23] is evident. We note that our method differs from that approach in that the optimization of the input density is achieved by us through a variational ETF method, which does not require a step-by-step matrix diagonalization. While our focus in this Letter is on jellium models for metal clusters, the good agreement between our results and those obtained via KA-LDA jellium calculations [7,10,11,24] suggests that it would be worthwhile to explore the application of our method to more general electronic structure calculations extending beyond the jellium model.

3. Results

3.1. Electron affinities and borders of stability

The smooth multiple electron affinities $\tilde{A}_Z$ prior to shell corrections are defined as the difference in the total energies of the clusters

$$\tilde{A}_Z=\tilde{E}(vN, vN+Z-1)-\tilde{E}(vN, vN+Z),$$

where N is the number of atoms, v is the valency and Z is the number of excess electrons in the cluster (e.g., first and second affinities correspond to $Z=1$ and $Z=2$, respectively). vN is the total charge of the positive background. Applying the shell correction ΔE_{sh} defined earlier, we calculate the full electron affinity as

$$A_Z^{sh}-\tilde{A}_Z=\Delta E_{sh}(vN, vN+Z-1)$$
$$-\Delta E_{sh}(vN, vN+Z).$$

A positive value of the electron affinity indicates stability upon attachment of an extra electron. Fig. 1 displays the smooth, as well as the shell corrected, first and second electron affinities for sodium clusters with $N<100$, calculated for spherical jellium. Since shell effects are expected to be overestimated by the spherical jellium, we also include (see fig. 1b) shell corrected results for A_1, calculated for *triaxially*

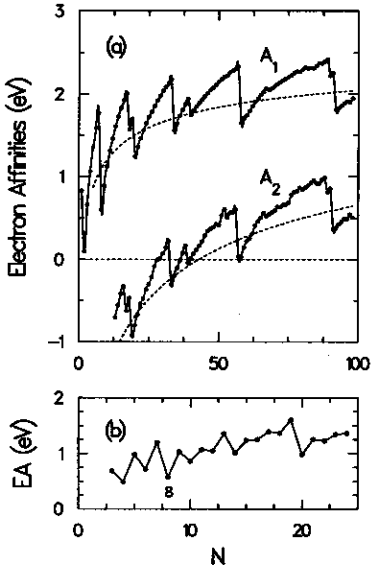

Fig. 1. (a) Calculated first (A_1) and second (A_2) electron affinities of sodium clusters (modeled as spheres) as a function of the number of atoms N. Both their *smooth* part (dashed lines) and the shell-corrected affinities (solid circles) are shown. (b) Electron affinity A_1 calculated for triaxially deformed Na_N droplets.

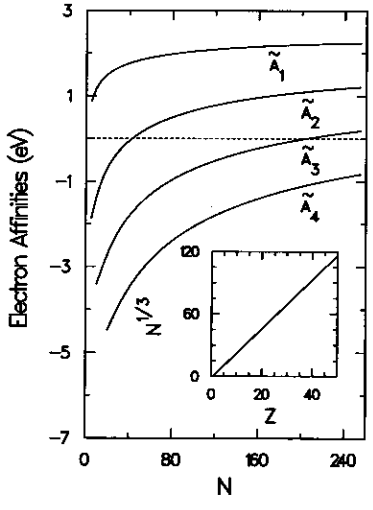

Fig. 2. Calculated smooth electron affinities $\tilde{A}_Z$, $Z=1$–4, for sodium clusters (modeled as spheres) as a function of the number of atoms N (Z is the number of excess electrons). Inset: The electron drip line for sodium clusters. Clusters stable against spontaneous electron emission are located above this line. While as seen from fig. 1a for spherical geometry, shell effects influence the border of stability, shell-corrected calculations including deformations yield values close to the drip line shown in the inset, which was obtained from the smooth contributions.

deformed [#3] jellium shapes. These latter results exhibit odd–even oscillations and shell and subshell closure effects in agreement with experimental observations [6] (see footnote 2).

Note that $\tilde{A}_2$ in fig. 1a becomes positive above a certain critical size, implying that the second electron in double negatively charged sodium clusters with $N<N_{cr}^{(2)}=43$ might not be stably attached. To predict the critical cluster size $N_{cr}^{(Z)}$, which allows stable attachment of Z excess electrons, we calculated the smooth electron affinities of sodium clusters up to $N=255$ for $1\leqslant Z\leqslant 4$, and display the results in fig. 2. We observe that $N_{cr}^{(3)}=205$, while $N_{cr}^{(4)}>255$.

The similarity of the shapes of the curves in fig. 2, and the regularity of distances between them, suggest that the smooth electron affinities can be fitted by a general expression of the form:

$$\tilde{A}_Z=\tilde{A}_1-\frac{(Z-1)e^2}{R+\delta}$$

$$=W-\beta\frac{e^2}{R+\delta}-\frac{(Z-1)e^2}{R+\delta}, \qquad (1)$$

where the radius of the positive background is $R=r_sN^{1/3}$. From our fit, we find that the constant W corresponds to the bulk work function. In all cases, we find $\beta=\frac{5}{8}$, which suggests a close analogy with the classical model of the image charge [26,27]. For the spill-out parameter, we find a weak size dependence as $\delta=\delta_0+\delta_2/R^2$. The contribution of δ_2/R^2, which depends on Z, is of importance only for smaller sizes and does not affect substantially the critical sizes (where the curve crosses the zero line), and consequently δ_2 can be neglected in such estimations. Using the values obtained by us for $\tilde{A}_1$ of sodium clusters (namely, $W=2.9$ eV which is also the value obtained by KS-LDA calculations for an infinite planar surface [28], $\delta_0=1.16$ au; with $r_s=4.00$ au), we find for the critical sizes when the lhs of eq. (1)

[#3] KS-LDA calculations (for the first IP and first EA), restricted to *spheroidally* (axially symmetric) deformed jellium droplets with $N\leqslant 40$ were given in ref. [11].

is set equal to zero, $N_{cr}^{(2)}=44$, $N_{cr}^{(3)}=202$, $N_{cr}^{(4)}=554$, and $N_{cr}^{(5)}=1177$, in good agreement with the values obtained directly from fig. 2.

The curve that specifies $N_{cr}^{(Z)}$ in the (Z, N) plane defines the border of stability for spontaneous electron decay. In nuclei, such borders of stability against spontaneous proton or neutron emission are known as nucleon drip lines [20]. For the case of sodium clusters, the electron drip line is displayed in the inset of fig. 2.

The methodology and conclusions of our study extend to other materials as well. Thus given a calculated or measured bulk work function W, and a spill-out parameter (δ_0 typically of the order of 1–2 au, and neglecting δ_2), one can use eq. (1), with $\tilde{A}_Z=0$, to predict critical sizes for other materials. Our calculations for potassium ($r_s=4.86$ au) give fitted values $W=2.6$ eV (compared to a KS-LDA value of 2.54 eV for a semi-infinite planar surface with $r_s=5.0$ au [28]) and $\delta_0=1.51$ au for $\delta_2=0$, yielding $N_{cr}^{(2)}=33$, $N_{cr}^{(3)}=152$, and $N_{cr}^{(4)}=421$. For a trivalent metal, i.e. aluminum ($r_s=2.07$ au), for which our fitted values are $W=3.65$ eV (compared to a KS-LDA value of 3.78 eV for a semi-infinite plane surface, with $r_s=2.0$ au [28]) and $\delta_0=1.86$ au for $\delta_2=0$, we find $N_{cr}^{(2)}=40$ (121 electrons), $N_{cr}^{(3)}=208$ (626 electrons), and $N_{cr}^{(4)}=599$ (1796 electrons).

3.2. Metastability against electron autodetachment

The multiply charged anions with negative affinities do not necessarily exhibit a positive total energy. To illustrate this point, we display in fig. 3 the calculated total energies per atom ($\tilde{E}(N, Z)/N$) as a function of excess charge (Z) for clusters containing 30, 80 and 240 sodium atoms. These sizes allow for exothermic attachment of maximum one, two or three excess electrons, respectively.

As was the case with the electron affinities, the total energy curves in fig. 3 show a remarkable regularity, suggesting a parabolic dependence on the excess charge. To test this conjecture, we have extracted from the calculated total energies the quantities $g(N, Z)=G(N, Z)/N$, where $G(N, Z)=[\tilde{E}(N, Z)-\tilde{E}(N, 0)]/Z+\tilde{A}_1(N)$, and have plotted them in the inset of fig. 3 as a function of the excess negative charge Z. The dependence is linear to a remarkable extent;

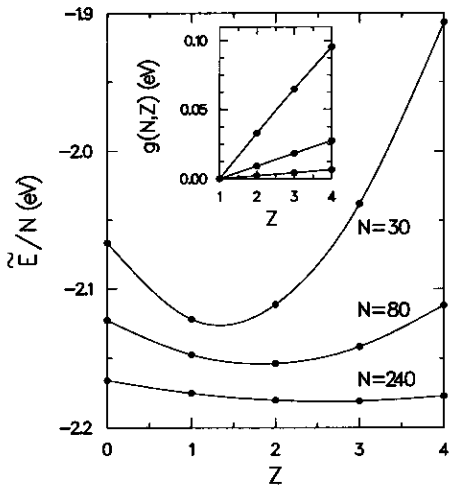

Fig. 3. Calculated smooth total energy per atom as a function of the excess negative charge Z for the three families of sodium clusters with $N=30$, $N=80$ and $N=240$ atoms. As the straight lines in the inset demonstrate, the curves are parabolic. We find that they can be fitted by eq. (2). See text for an explanation of how the function $g(N, Z)$ was extracted from the calculations.

for $Z=1$ all three lines cross the energy axis at zero. Combined with the results on the electron affinities, this indicates that the total energies have the following dependence on the excess number of electrons (Z):

$$\tilde{E}(Z)=\tilde{E}(0)-\tilde{A}_1 Z+\frac{Z(Z-1)e^2}{2(R+\delta)}, \qquad (2)$$

where the dependence on the number of atoms in the cluster is not explicitly indicated.

This result is remarkable in its analogy with the classical image-charge result of van Staveren et al. [27]. Indeed, the only difference amounts to the spill-out parameter δ_0 and to the weak dependence on Z through δ_2. This additional Z-dependence is already negligible for the case of 30 sodium atoms.

For metastable multiply charged cluster anions (namely those with $\tilde{E}(N, Z)<0$, but $\tilde{A}_Z<0$, for $Z>1$), electron emission (autodetachment) will occur via tunneling through a barrier (shown in fig. 4). However, to estimate the electron emission reliably, it is necessary to correct the LDA effective potential for self-interaction effects. We performed a self-interaction correction of the Amaldi type [12] for the Hartree term and extended it to the exchange-cor-

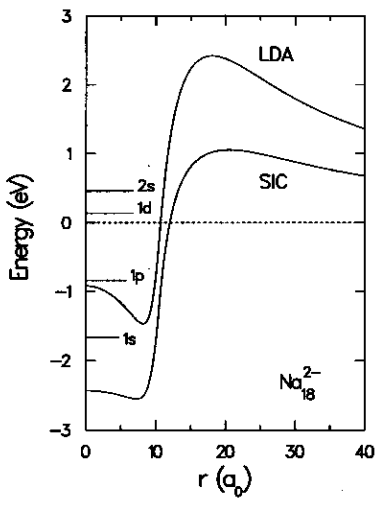

Fig. 4. The LDA and the corresponding self-interaction corrected (SIC) potential for the metastable Na_{18}^{2-} cluster. The single-particle levels of the SIC potential are also shown. Unlike the LDA, this latter potential exhibits the correct asymptotic behavior. The 2s and 1d electrons can be emitted spontaneously by tunneling through the Coulombic barrier of the SIC potential. Distances in units of the Bohr radius, a_0.

relation contribution to the total energy as follows: $E_{xc}^{SIC}[\rho]=E_{xc}^{LDA}[\rho]-N_e E_{xc}^{LDA}[\rho/N_e]$, where $N_e=\nu N+Z$ is the total number of electrons. This self-interaction correction is akin to the orbitally averaged potential method [12]. Minimizing the ETF-SIC energy functional for the parameters $\{\gamma_i\}$, we obtained the effective SIC potential for Na_{18}^{2-} shown in fig. 4, which exhibits the physically correct asymptotic behavior [#4].

The spontaneous electron emission through the Coulombic barrier is analogous to that occurring in proton radioactivity from neutron-deficient nuclei [29], as well as in alpha-particle decay. The transition rate is $\lambda=\ln 2/T_{1/2}=\nu P$, where ν is the attempt frequency and P is the transmission coefficient calculated by the WKB method (for details, cf. ref. [29]). For the 2s electron in Na_{18}^{2-} (cf. fig. 4), we find $\nu=0.73\times10^{15}$ Hz and $P=4.36\times10^{-6}$, yielding $T_{1/2}=2.18\times10^{-10}$ s. For a cluster size closer to the drip line (see fig. 2), e.g. Na_{35}^{2-}, we find $T_{1/2}=1.13$ s.

[#4] We emphasize that while the effective potentials are significantly different when SIC is used, other quantities, such as the total energy, IPs, and EAs are only slightly altered by SIC as shown in ref. [12], and by our own calculations.

3.3. Fission energetics for doubly charged anions

Since fission channels may compete with the spontaneous electron emission, we calculated the dissociation energies, $\Delta_P=E_{sh}(Na_P^-)+E_{sh}(Na_{N-P}^-)-E_{sh}(Na_N^{2-})$, as a function of parent size N and daughter products P and $N-P$, for doubly charged anions modeled as spherical as well as triaxially deformed jellium droplets. The dissociation energies Δ_f for the most favorable channels, i.e. for the smallest Δ_P for a given N, are displayed in fig. 5. As seen, magic parents are the least favored to fission, exhibiting typically endothermic behavior. All favorable channels contain at least one magic fragment. For spherical droplets, pronounced local minima correspond to open-shell parents. The magnitudes of these minima in Δ_f are reduced when deformations are included since the latter stabilize the open-shell parents. The local minima of Δ_f for the doubly anionic parents remain exothermic even for sizes as large as $N=100$ atoms when spherical symmetry is assumed, while our results including deformations suggest that for Na_N^{2-} clusters, due to a strong suppression of the local minima, the fission channel becomes exothermic (and may compete with the electron-emission one) only for $N\leqslant30$. Similar trends are found by us [25] in the case of deformed cationic Na_N^{2+} clusters,

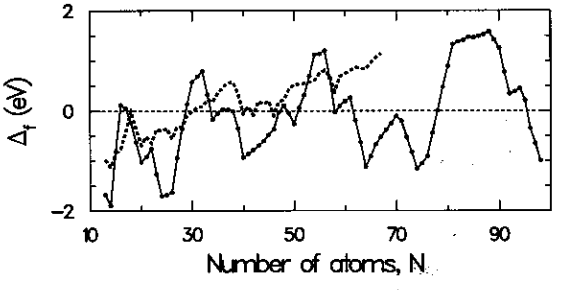

Fig. 5. Solid circles: Shell correction method (SCM) results for the dissociation energies Δ_f for the most favorable fission channel for doubly charged anionic parents Na_N^{2-} when the spherical jellium is used. Results including triaxial deformations are shown by a thick dashed line.

in agreement with experimental observations [4].

4. Conclusion

The stability and electron decay channels of multiply charged anionic metal clusters were studied using the uniform jellium background model and the local density approximation, with self-interaction corrections when necessary. Shell effects were introduced using a new shell-correction method, which is based on the same principle as the Strutinsky approach familiar from nuclear physics. Singly charged anions were shown to be stable for all sizes, but multiply charged negative ions are stable against spontaneous electron decay only above certain critical sizes. Below the border of stability, the anions are metastable against electron tunneling through a Coulombic barrier. Lifetimes for such decay processes were estimated. Fission channels which compete with the electron autodetachment were studied for the case of doubly charged anions.

Confrontation of our predictions with experiment would require measurements on mass-selected multiply negatively charged metal clusters. A method for generating such clusters may involve fragmentation (via heating or collisions) of large charged droplets produced by a liquid metal source.

In this context, it is interesting to observe that the results presented in this Letter are relevant to the problem of charging a zero-dimensional electron gas (0DEG) which forms in Coulomb islands and quantum dots, as well as other nanodevices that have been recently fabricated [30,31].

Acknowledgement

This research was supported by a grant from the US Department of Energy (Grant No. AG05-86ER45234).

References

[1] C. Coulomb, Mémoires de l'Académie (1786) p. 67 ff; (1787) p. 452;
M. Faraday, Experimental research in electricity (1839) (Dover, New York, 1965) Vol. I, pp. 360 ff.
[2] W.A. de Heer, W.D. Knight, M.Y. Chou and M.L. Cohen, Solid State Phys. 40 (1987) 93.
[3] Fifth International Symposium on Small Particles and Inorganic Clusters, Konstanz, 1990, Z. Physik D 19 (1991); 20 (1991).
[4] C. Bréchignac, Ph. Cahuzac, F. Carlier and M. de Frutos, Phys. Rev. Letters 64 (1990) 2893;
C. Bréchignac, Ph. Cahuzac, F. Carlier, J. Leygnier and A. Sarfati, Phys. Rev. B 44 (1991) 11386.
[5] T.P. Martin, U. Näher, H. Göhlich and T. Lange, Chem. Phys. Letters 196 (1992) 113, and references therein.
[6] J.G. Eaton, L.H. Kidder, H.W. Sarkas, K.M. McHugh and K.H. Bowen, in: Nuclear physics concepts in the study of atomic cluster physics, eds. R. Schmidt et al., Lecture notes in physics, Vol. 404 (Springer, Berlin, 1992) p. 291.
[7] W. Ekardt, Phys. Rev. B 29 (1984) 1558.
[8] U. Röthlisberger and W. Andreoni, J. Chem. Phys. 94 (1991) 8129.
[9] R.N. Barnett, U. Landman and G. Rajagopal, Phys. Rev. Letters 67 (1991) 3058; 69 (1992) 1472.
[10] L.C. Balbás, A. Rubio and J.A. Alonso, Chem. Phys. 120 (1988) 239.
[11] Z. Penzar and W. Ekardt, Z. Physik D 17 (1990) 69.
[12] J.P. Perdew and A. Zunger, Phys. Rev. B 23 (1981) 5048.
[13] Ll. Serra, F. Garcias, M. Barranco, J. Navarro, C. Balbás and A. Mañanes, Phys. Rev. B 39 (1989) 8247.
[14] M. Brack, Phys. Rev. B 39 (1989) 3533.
[15] C. Yannouleas, E. Vigezzi and R.A. Broglia, Phys. Rev. B 47 (1993) 9849;
C. Yannouleas, Chem. Phys. Letters 193 (1992) 587;
C. Yannouleas and R.A. Broglia, Phys. Rev. A 44 (1991) 5793.
[16] C.H. Hodges, Can. J. Phys. 51 (1973) 1428.
[17] O. Gunnarsson and B.I. Lundqvist, Phys. Rev. B 13 (1976) 4274.
[18] Å. Bohr and B.R. Mottelson, Nuclear structure, Vol. 2 (Benjamin, Reading, 1975).
[19] V.M. Strutinsky, Nucl. Phys. A 95 (1967) 420; A 122 (1968) 1.
[20] Ph.J. Siemens and A.S. Jensen, Elements of nuclei (Addison-Wesley, New York, 1987).
[21] J. Harris, Phys. Rev. B 31 (1985) 1770.
[22] M.W. Finnis, J. Phys. Condens. Matter 2 (1990) 331.
[23] E. Zaremba, J. Phys. Condens. Matter 2 (1990) 2479.
[24] M.Y. Chou, A. Cleland and M.L. Cohen, Solid State Commun. 52 (1984) 645.
[25] C. Yannouleas and U. Landman, to be published.
[26] D.M. Wood, Phys. Rev. Letters 46 (1981) 749.
[27] M.P.J. van Staveren, H.B. Brom, L.J. de Jongh and Y. Ishii, Phys. Rev. B 35 (1987) 7749.
[28] J.P. Perdew and Y. Wang, Phys. Rev. B 38 (1988) 12228.
[29] S. Hofmann, in: Particle emission from nuclei, Vol. 2, ed. D.N. Poenaru and M.S. Ivascu (CRC Press, Boca Raton, 1989) p. 25.
[30] M.A. Kastner, in: Physics Today 46 (1993) 24.
[31] H. Grabert and M.H. Devoret, eds., Single charge tunneling (Plenum Press, New York, 1992).
[32] A. Rubio, L.C. Balbas and J.A. Alonso, Physica B 167 (1990) 19.